

J.J. Brey J. Marro J. M. Rubí M. San Miguel (Eds.)

# 25 Years of Non-Equilibrium Statistical Mechanics

Proceedings of the XIII Sitges Conference,  
Held in Sitges, Barcelona, Spain,  
13–17 June 1994



Springer

# Finite-Size Effects in the Kardar-Parisi-Zhang Equation

Raul Toral <sup>1</sup>, Bruce Forrest <sup>2</sup>

<sup>1</sup>Departament de Física, Universitat de les Illes Balears, 07071-Palma de Mallorca, Spain,

<sup>2</sup>Institut für Polymere, E.T.H. Zürich, CH-8092 Zürich, Switzerland

**Abstract:** On the basis of a perturbative solution we study the numerical importance of finite-size effects in the Kardar-Parisi-Zhang equation for surface growth. The crossover behaviour between linear and non-linear regimes is studied numerically using convenient finite size scaling expressions.

In the exciting field of non-equilibrium phenomena, much attention has been drawn recently to the problem of growth of random surfaces[1]. It has become clear that many different growth models share similar features such as scaling exponents and scaling functions and can thus be considered as belonging to the same *universality class*. The Kardar-Parisi-Zhang (hereafter referred to as KPZ) equation[2] is a prototype model for those systems in which the interface growth is driven by an external flux of particles. In the KPZ model, the surface height  $h(\mathbf{r}, t)$  on top of location  $\mathbf{r}$  of a  $d$ -dimensional substrate satisfies a stochastic random equation:

$$\frac{\partial h(\mathbf{r}, t)}{\partial t} = \nu \nabla^2 h(\mathbf{r}, t) + \frac{\bar{\lambda}}{2} (\nabla h)^2 + \eta(\mathbf{r}, t) \quad (1)$$

Every term in this equation models a physical phenomenon contributing to the surface evolution:  $\nu$ ,  $\bar{\lambda}$  and  $D$  are parameters describing, respectively, surface relaxation, lateral growth and the effect of noise. This noise term aims to describe the random fluctuations in the incident flux of particles and is assumed to be a Gaussian random process of mean zero and correlations:

$$\langle \eta(\mathbf{r}, t) \eta(\mathbf{r}', t') \rangle = 2D \delta(\mathbf{r} - \mathbf{r}') \delta(t - t') \quad (2)$$

A convenient measure of the surface roughness is given by averaging the spatial fluctuations over different realizations of the noise:

$$w(t) = \sqrt{\langle \bar{h}^2 - \bar{h}^2 \rangle} \quad (3)$$

Where the bar and the brackets denote the spatial and noise averages, respectively. Several time regimes can be found in the time evolution of the surface roughness. They can be summarized as follows:

(i) For very early times, the noise term dominates since its contribution to the equation grows as the square root of time. It is easy to find that the surface roughness grows in this time regime as  $w(t) \sim t^{1/2}$ .

(ii) For intermediate times, the linear term is the main contribution. The linear case ( $\bar{\lambda} = 0$ ) is the Edwards–Wilkinson model[3] for which one can find easily that the surface roughness behaves as  $w(t) = t^{\beta_0}$ . The value for  $\beta_0$  depends on the dimension of the substrate:  $\beta_0 = 1/4$  for one-dimensional surfaces,  $\beta_0 = 0$  (logarithmic growth) for the two-dimensional case.

(iii) For late times, the contribution of the relevant non-linear term becomes the dominant one and the surface roughness growth is characterized by a behaviour  $w(t) = t^\beta$ .

(iv) For very late times and finite substrate length  $L$ , the roughness saturates to a value  $w(t \rightarrow \infty, L) \sim L^\zeta$ .

Of course, in an experiment or in a numerical simulation, the transition between the different regimes is not sharp and different crossover behaviours can be observed. For the transition between non-linear (iii) and saturation (iv) regimes, a scaling law has been derived[4]:

$$w(t, L) = L^\zeta F(tL^{-z}) \quad (4)$$

$\zeta$  and  $z$  are the *roughness* and *dynamic* exponents, respectively. In order to recover the known limiting behaviours, the scaling function  $F(x)$  behaves as  $F(x) \sim x^{z/\zeta}$  (hence  $\beta = z/\zeta$ ) for  $x \ll 1$  and approaches a constant for large  $x$ . Galilean invariance implies the exact relation  $z + \zeta = 2$  independently of dimension[5]. In one-dimensional substrates, a fluctuation–dissipation theorem[6] yields the exact values for the exponents  $z = 3/2$ ,  $\zeta = 1/2$ ,  $\beta = 1/3$ . It is interesting to notice that in the absence of non-linear terms a similar scaling relation holds but with different values for the exponents, namely  $w(t, L) = L^{\zeta_0} F_0(tL^{-z_0})$ ,  $\zeta_0 = 1/2$ ,  $z_0 = 2$ . So, in order to measure the correct crossover exponents and functions for non-linear to saturation behaviour, it is important to make sure that non-linear effects have fully developed before the saturation regime has started.

The precise knowledge of the dynamical exponents is very important since it allows a detailed characterization of the universality classes. Many numerical studies have been devoted to checking the scaling relations and to computing as accurately as possible the values for the scaling exponents[7]. Since a numerical simulation will deal necessarily with a system of finite-size, it is very important to analyze carefully the effect of finite-size effects in the different time regimes specified above and also on the crossover behaviour from one regime to another[8]. In this paper, we present a detailed study of the relevance that finite-size effects have in a numerical simulation of the KPZ equation and we show how it is possible, using convenient finite-size scaling forms, to compute the dynamical exponents that characterize the crossover from linear (ii) to non linear behaviour (iii).

It is possible to reparametrize the surface field  $h \rightarrow (\nu/2D)^{1/2}h$  and time  $t \rightarrow \nu t$  to obtain a somewhat simpler version of the KPZ equation:

$$\frac{\partial h(\mathbf{r}, t)}{\partial t} = \nabla^2 h(\mathbf{r}, t) + \frac{\lambda}{2} (\nabla h)^2 + \eta(\mathbf{r}, t) \quad (5)$$

where  $\lambda = (2D/\nu^3)^{1/2}\bar{\lambda}$  and the noise term satisfies  $\langle \eta(\mathbf{r}, t)\eta(\mathbf{r}', t') \rangle = \delta(\mathbf{r} - \mathbf{r}')\delta(t - t')$ . This reparametrization of the equation is achieved by simply setting  $2D = \nu = 1$  in the original KPZ equation. In the numerical studies, typically one introduces a lattice discretization of the space variable  $r_j = r_0 + ja_0$  (we restrict ourselves to one-dimensional systems from now on), so introducing a set of discrete variables  $h_j(t) = h(r_j, t)$  in terms of which we write:

$$\frac{\partial h_j(t)}{\partial t} = (h_{j+1} + h_{j-1} - 2h_j) + \frac{\lambda}{2} \left( \frac{h_{j+1} - h_{j-1}}{2a_0} \right)^2 + \eta_j(t), \quad (6)$$

Periodic boundary conditions are usually assumed in order to avoid edge effects and the linear spacing  $a_0$  is set to the unit length,  $a_0 = 1$ . It is possible to obtain the solution of the corresponding linear model ( $\lambda = 0$ ) as formulated on the lattice to find that the surface roughness  $w_{(0)}$  in this case is given by:

$$w_{(0)}^2(t, L) = \frac{1}{L} \sum_{k=1}^{L-1} \frac{1 - \exp(-2\alpha_k t)}{2\alpha_k}. \quad (7)$$

where  $\alpha_k \equiv 4 \sin^2(\pi k/L)$ . For infinite size, this linear solution behaves asymptotically as:

$$w_{(0)}^2(t, L \rightarrow \infty) = \left( \frac{t}{2\pi} \right)^{1/2} \left( 1 - \frac{1}{32t} \right) \quad (8)$$

(this expression has an error of less than 0.1% for  $t \geq 1$ ) and, consequently, the dynamical exponent is  $\beta_0 = 1/4$  as anticipated. This linear solution has a strong  $L$ -dependence as it is shown in figure (1) where we plot, in a double logarithmic scale, the time evolution of the surface roughness versus time for different system sizes. According to the above asymptotic solution this plot should yield a straight line of slope 1/2. However, finite values of  $L$  have the effect of bending the curves so producing *effective* exponents which are smaller than the true exponents.

Similar conclusions can be drawn in the non-linear case. Here we do not know the exact solution but we can make use of a perturbative expansion in  $\lambda$  to find the leading correction (which is second order in  $\lambda$ ) to the surface roughness as[8]:

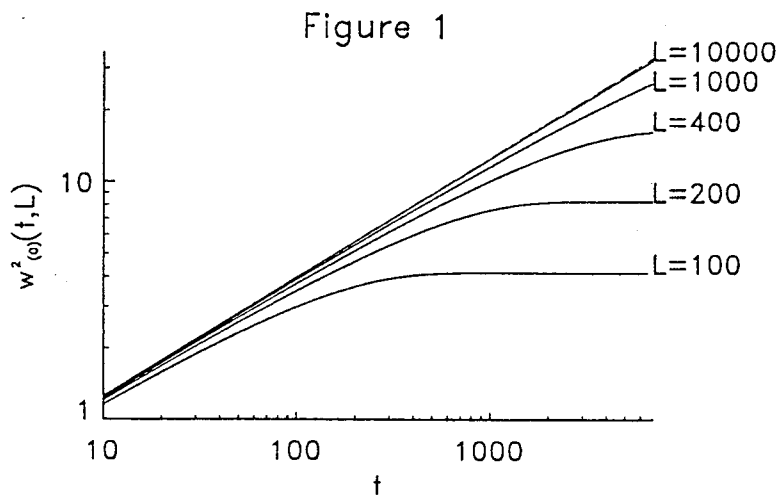


Fig. 1. Square of the surface roughness,  $w_{(0)}^2$ , for the linear solution (equation 9), as a function of system size  $L$ . For long times, the roughness saturates to a value that depends on  $L$ . For intermediate times, the slopes of the curves yield effective dynamical exponents less than the true asymptotic value  $\beta_0 = 1/4$ . The dashed line is the corresponding solution in the limit  $L \rightarrow \infty$ .

$$\begin{aligned}
 w^2(t, L)^{(2)} = & w_{(0)}^2(t, L) \\
 & + \frac{\lambda^2}{16L^2} \sum_{k=1}^{L-1} e^{-2\alpha_k t} \sum_{k_1=0}^{L-1} \cos^2(\pi(k-k_1)/L) \times \left\{ \cos^2(\pi k_1/L) \right. \\
 & \times [f(a, a, t) - f(a, b, t) - f(a, c, t) + f(a, d, t)] \\
 & + \cot(\pi k/L) \sin(2\pi k_1/L) \\
 & \left. \times [f(a, -a, t) - f(a, -b, t) + f(a, c, t) - f(a, d, t)] \right\} \\
 & + o(\lambda^4)
 \end{aligned} \tag{9}$$

with  $a = -\alpha_{k_1} - \alpha_{k-k_1} + \alpha_k$ ,  $b = -\alpha_{k_1} + \alpha_{k-k_1} + \alpha_k$ ,  $c = \alpha_{k_1} - \alpha_{k-k_1} + \alpha_k$ ,  $d = \alpha_{k_1} + \alpha_{k-k_1} + \alpha_k$  and  $f(x, y, t) = \frac{x e^{(x+y)t} - (x+y)e^{xt+y}}{xy(x+y)}$  (and appropriate limits assumed for the case  $xy(x+y) = 0$ ). Comparing with numerical simulations we see that the perturbative solution offers an accurate approximation for  $\lambda = 0.5$  up to  $t \approx 6000$  and for  $\lambda = 1$  for  $t \lesssim 1000$  (see figure (2)).

We can use the perturbative solution at  $\lambda = 0.5$  to examine the effect of finite  $L$  on the solution in a similar fashion to the linear case studied above. In figure (3) we have plotted in a double logarithmic scale the time evolution of the roughness  $w^2(t, L)^{(2)}$  as given by the second-order perturbation, equation (9), as a function of system size  $L$ . It is obvious from this figure that when dealing

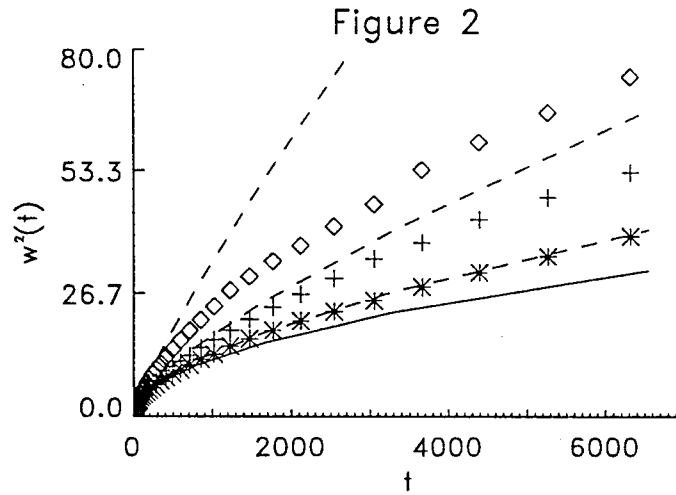


Fig. 2. Comparison of a numerical integration of the KPZ equation (symbols) for a system size  $L = 10^4$  with the perturbative solution given in equation (9) (dashed lines) for the cases  $\lambda = 2, 1, 0.5$  from top to bottom, respectively. The solid line is the exact linear solution

with finite system sizes the exponents obtained from these log-log plots should be considered only as effective exponents. Only for  $L \gtrsim 10^4$  the relative error in the roughness is less than 1% up to times  $t \simeq 6000$

One can obviously question the validity of the perturbation expansion to obtain dynamical exponents, but it is important to point out that the finite-size effects worsen with increasing  $\lambda$ . This is obvious from figure (4) where we have plotted as a function of  $t$  the relative weight of the second-order term in the expansion at finite  $L$  compared to its asymptotic value ( $L \rightarrow \infty$ ) as measured by the ratio  $R \equiv w^2(t, L)^{(2)}/w^2(t, \infty)^{(2)}$  for  $\lambda = 0$  and  $0.5$  at  $L = 1000$  and  $10000$ . Upon switching from  $\lambda = 0$  to  $\lambda = 0.5$  the ratio  $R$  is clearly seen to fall even further away from unity ( $R = 1$  implies no finite-size effects). One can conclude that, at least for  $d = 1$  and within the range of validity of the perturbative solution, the minimum value of  $L$  required in the linear case to avoid finite-size effects only provides a lower bound for  $\lambda \neq 0$ .

We turn now to the effect of finite-size effects in the crossover from linear to non-linear behaviour (regimes (ii) to (iii) above). For this crossover, two different scaling forms have been advocated. In a one-loop renormalization-group (RG) calculation Natterman and Tang (NT) found[9]:

$$w^2(t, L) = L^{2\zeta_0} f\left(\frac{t}{t_c}, \frac{L}{\xi_c}\right). \quad (10)$$

where the crossover time satisfies  $t_c \sim \xi_c^{z_0}$ . In the limit of small  $\lambda$ , one has the dependence:  $\xi_c \sim \lambda^{-2}$  and  $t_c \sim \lambda^{-4}$ . On the other hand, Grossmann, Guo, Grant

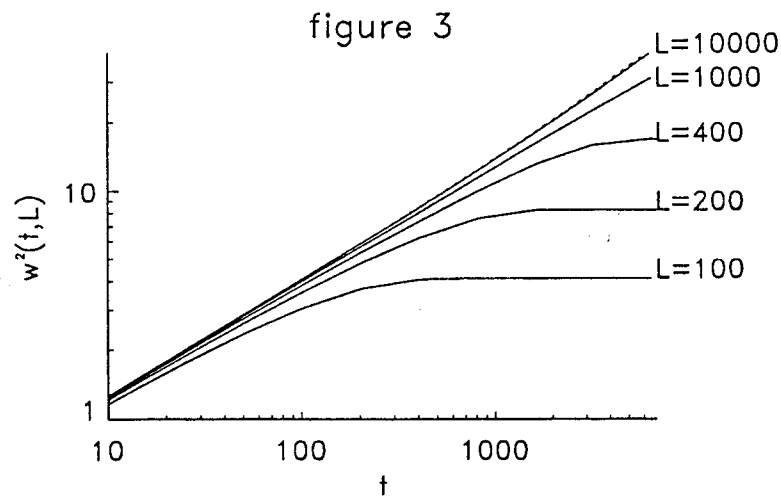


Fig. 3. Same as figure 1, but using the perturbative solution given in equation (9). Notice that again finite size effects show up as effective exponents in this log-log plot.

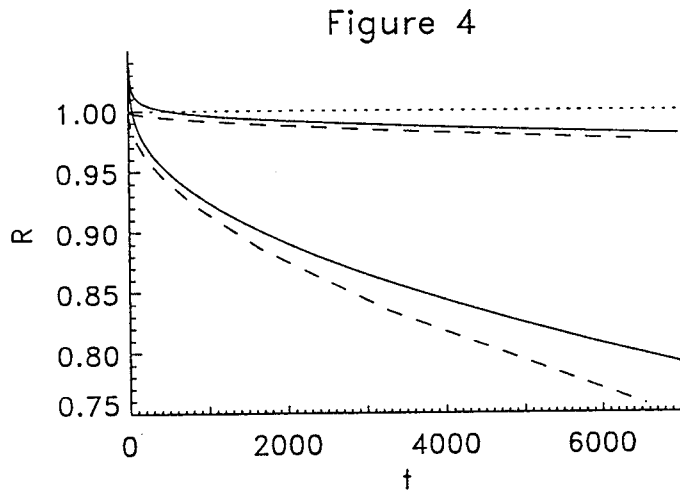


Fig. 4. Ratio  $R = w^2(t, L)^{(2)} / w^2(t, \infty)^{(2)}$  from the second-order perturbation expression (equation (9)) as a function of time  $t$  for  $\lambda = 0$  (solid lines) and  $\lambda = 0.5$  (dashed lines) for two different values of  $L = 1000$  (two lower lines), and  $L = 10000$  (upper lines). If there were no finite size effects,  $R$  would take the constant value  $R = 1$  (dotted line).

(GGG) proposed the form[10]:

$$w^2(t, L) = t^{2\beta_0} f\left(\frac{t}{L^{z_0}}, \frac{t}{\xi_c^{z_0}}\right). \quad (11)$$

and they made the ansatz that the crossover length scales as  $\xi_c \sim \lambda^{-\phi}$  and on the basis of their numerical findings predicted the value  $\phi = 3$ , at variance with the value of NT. The data analysis of GGG that led to  $\phi = 3$  used the asymptotic  $L \rightarrow \infty$  form for the scaling relations, although in their numerical simulation these authors had used system sizes  $L = 10^3$  and times  $t = 10^4$  for which there are clear finite-size effects (see figure 3). It seems necessary, then, to reanalyze the problem using finite-size expressions. One can reduce the two proposed expressions to a similar form if one considers the nonlinear-to-saturation regime, when the crossover to nonlinear growth has already taken place. This limit requires a system size  $L$  larger than the crossover length  $\xi_c$  and also times larger than the crossover time  $t_c$ . One can show that, in this case, the expressions of NT and GGG reduce to the similar form:

$$w^2(t, L) = Lf(t\lambda^{\frac{\phi}{4}}L^{-3/2}) \quad (12)$$

where  $\phi = 3$  according to GGG and  $\phi = 4$  according to NT. In order to check this expression, we have plotted in figure (5)  $w^2(t, L)/L$  vs.  $t\lambda^{\phi/4}L^{-3/2}$ . It appears that choice of  $\phi = 3$  gives a significantly superior data-collapse to that of  $\phi = 4$ .

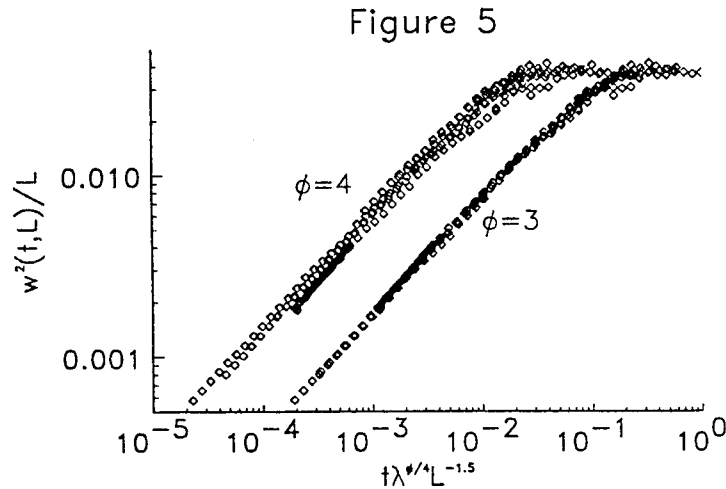


Fig. 5. Check of the finite-size scaling form, equation (11), with two different values for the exponent  $\phi$ . Several simulations have been performed for system sizes  $L = 100, 500, 1000$  and  $10000$  and values of  $\lambda$  ranging from  $\lambda = 2$  to  $\lambda = 10$ . For the purpose of clarity, the data set with  $\phi = 4$  has been shifted parallel to the horizontal axis.

To explain the failure of the RG calculation of Natterman and Tang to describe the simulation data one can argue that the specific RG expressions are only valid asymptotically in the limit  $\lambda \rightarrow 0, L \rightarrow \infty$  and that our simulations have



not entered yet this asymptotic regime. Also, we note that the discretization in equation (5) can only be expected to reproduce the continuum behaviour used in the RG calculations if the mesh size  $a_0$  is much less than the basic length scale  $\nu^3/\lambda^2 D$  inherent in (1). In our parametrization, this corresponds to  $\lambda < \sqrt{2}$ . However, our results for the finite-size analysis (which favoured  $\phi = 3$ ) were obtained with  $2 \leq \lambda \leq 10$ . Simulations at smaller values of  $\lambda$  (and therefore extended to much longer times in order to allow the development of non-linear effects) would be useful to resolve this issue.

## References

- [1] Reviews on kinetic roughening in surface growth models can be found in: J. Krug and H. Spohn, in *Solids Far From Equilibrium: Growth, Morphology and Defects*, edited by C. Godrèche, (Cambridge Univ. Press, Cambridge, England, 1991); *Kinetics of Ordering and Growth at Surfaces*, edited by M. Lagally (Plenum, New York, 1990), and references therein; T. R. Thomas, *Rough Surfaces* (Longman, London, 1982).
- [2] M. Kardar, G. Parisi, and Y.-C. Zhang, *Phys. Rev. Lett.* **56**, 889 (1986); E. Medina, T. Hwa, M. Kardar, and Y.-C. Zhang, *Phys. Rev. A* **39**, 3053 (1989).
- [3] S. F. Edwards and D. R. Wilkinson, *Proc. R. Soc. Lon. A* **381**:17 (1982).
- [4] F. Family and T. Vicsek, *J. Phys. A* **18**, L75 (1985). R. Jullien and R. Botet, *J. Phys. A* **18**, 2279 (1985).
- [5] P. Meakin, P. Ramanlal, L. M. Sander, and R. C. Ball, *Phys. Rev. A* **34**, 5091 (1986); J. Krug, *Phys. Rev. A* **36** 5465 (1987).
- [6] U. Dekker and F. Haake, *Phys. Rev. A* **11**, 2043 (1975).
- [7] K. Moser, J. Kertész, and D. E. Wolf, *Physica A* **178**, 215 (1991) and references therein.
- [8] B. Forrest and R. Toral, *J. Stat. Phys.* **70**, 703 (1993).
- [9] T. Nattermann and L-H. Tang, *Phys. Rev. A* **45**, 7156 (1992).
- [10] B. Grossmann, H. Guo and M. Grant, *Phys. Rev. A* **43**, 1727 (1991);